Proton Transfer and Proton Concentrations in Protonated Nafion Fuel Cell Membranes

D. B. Spry and M. D. Fayer*

Department of Chemistry, Stanford University, Stanford, California 94305

Received: April 21, 2009; Revised Manuscript Received: June 3, 2009

Proton transfer in protonated Nafion fuel cell membranes is studied using several pyrene derivative photoacids. Proton transfer in the center of the Nafion nanoscopic water channels is probed with the highly charged photoacid 8-hydroxypyrene-1,3,6-trisulfonate (HPTS). At high hydration levels, both the time-integrated fluorescence spectrum and the fluorescence kinetics of HPTS permit the determination of hydronium concentration of the interior of the water pools in Nafion. The proton transfer kinetics of HPTS in protonated Nafion at maximum hydration are identical to the kinetics displayed by HPTS in a 0.5 M HCl solution. The hydronium concentration near the water interface in Nafion is estimated with rhodamine-6G to be 1.4 M. Excited state proton transfer (ESPT) is followed in the nonpolar side chain regions of Nafion with the photoacid 8-hydroxy-*N*,*N*,*N*′,*N*′,*N*″,*N*″-hexamethylpyrene-1,3,6-trisulfonamide (HPTA). Excited state proton transfer of HPTA is possible in protonated Nafion only at the highest hydration level due to a relatively high local pH.

I. Introduction

Nafion is a commercially available perfluorinated polymer manufactured by DuPont that is widely used as a permselective membrane in polymer electrolyte fuel cells (PEFCs).[1] In a PEFC, hydrogen is oxidized at the anode to generate a supply of electrons and protons. The electrons travel through an external circuit to the cathode. Protons simultaneously diffuse through a polymer electrolyte membrane (PEM) to the cathode to complete the electrochemical circuit. The ability of the PEM to selectively allow protons to travel from the anode to the cathode, while preventing the passage of the reactant gases, is essential for the PEFC's operation.

Nafion consists of a nonpolar fluorinated backbone and a polar polyether side chain terminated by a sulfonic acid moiety. The difference in polarity of these two groups results in the formation of segregated hydrophobic and hydrophilic nanoscopic domains. As the water content of the membrane is increased, the hydrophilic domains swell in size and form an interconnected network of transmembrane channels. Above the percolation threshold, protons are able to pass completely through the PEM via the hydrophilic regions. The acidic proton of the sulfonic acid can be substituted for another general cation, M^+, which is denoted as M-Nafion.

The proton mobility of Nafion, as well as other permselective membranes, has been shown to be highly selective to both geometric and chemical composition of the hydrophilic network.[1] The rate of proton transport is very dependent upon the water concentration.[2,3] In normal operation, the Nafion membrane is dehydrated due to electro-osmotic drag from hydronium transport.[3] The hydrogen gas input stream is saturated with water to maintain satisfactory hydration necessary for proton diffusion. The water content of Nafion can be defined by a parameter, λ, which is equal to the number of water molecules per sulfonic acid unit ($\lambda = [H_2O]/[SO_3H]$). It has been found empirically that the proton conductivity increases linearly with λ.[3]

Among the first descriptions for the microscopic structure of Nafion was the cluster-network model by Gierke and Hsu.[4,5] It was speculated that the morphology of Nafion consists of ionic sulfonate clusters that are roughly spherical in shape, resembling reverse micelles, and are connected by narrow channels that permit protons to travel from one cluster to another. A large number of experimental[1,6−13] and theoretical[14−22] studies in the last several decades have been undertaken to elucidate the structure of Nafion. It does seem from the vast amount of data available today that the earliest model of Gierke and Hsu is an oversimplification for what appears to be a more complicated phase separation. Although a number of models exist, the common consensus is that the structure of Nafion depends largely on the volume fraction of water present. At low concentrations of water, there exists reverse micelle-like clusters, which are generally found in nearly all ionomers.[23] As the volume fraction of water is significantly increased, it is believed that the reverse micelle structures merge together to form a torous network that is above the percolation threshold.[1,24] At high water concentrations, water and protons can pass through the membrane.

As primitive as the cluster-network model may be, the key to its longevity is that it has a remarkable ability to describe a number of properties of Nafion.[1] In a previous publication,[25] we compared the excited-state proton transfer dynamics of a photoacid chromophore located in the water channels of sodium-substituted Nafion, Na-Nafion, to a model reverse micelle system of a similar chemical composition, aersol-OT (AOT). The AOT emulsions form well-defined water nanopools that are lined with sulfonate groups at the water-reverse micelle interface. The AOT reverse micelle interface is similar to what is thought to be the water interface in Nafion. Characterization studies[26−28] have related the size of AOT reverse micelles to the hydration level, or the number of waters per surfactant molecule, which is typically referred to as w_o. However, in this paper the hydration will be referred to as λ to be consistent with the standard notation for quantifying the water content in Nafion.[3] It was found that the proton transfer equilibria, proton transfer kinetics, as well as the anisotropy decay dynamics of the probe molecule were very similar when comparing measurements made in Nafion and AOT reverse micelles at the same value of λ.[25] Although AOT cannot form stable reverse micelles when the sulfonic acid groups are protonated, it will be useful throughout this work to

* Corresponding author. E-mail: fayer@stanford.edu.

10.1021/jp9036777 CCC: $40.75
Published on Web 07/02/2009

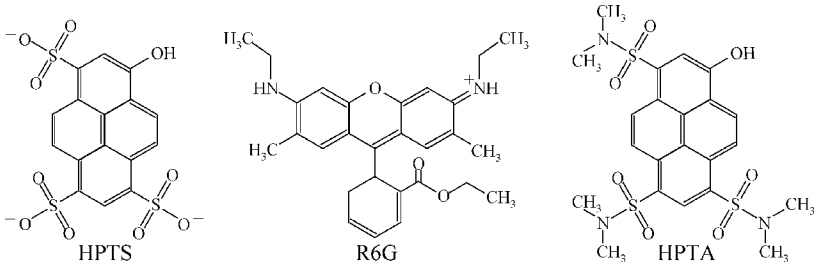

Figure 1. Structures and abbreviations for molecules referred to in this paper.

make comparisons to similar excited state proton transfer (ESPT) experiments performed in sodium-substituted AOT reverse micelles when drawing conclusions from the data collected from protonated Nafion.

Aside from its technological importance, Nafion is also interesting from a purely scientific perspective. It has long been known that the confinement of water on a nanometer length scale changes its physical properties through perturbation of the hydrogen bonding network.[29,30] Aqueous chemistry occurs in nanoscopic pores in a wide range of biological and catalytic systems. The traditional model systems used to study nanoconfined water, reverse micelles, have a pH-dependent phase diagram and typically cannot form stable structures with an extremely acidic water core. Therefore, Nafion provides the opportunity to study proton transfer dynamics in nanoconfined water with a high proton concentration.

Infrared spectroscopy has been an invaluable tool in recent years for studying the perturbed nature of water in nanoconfined systems. Steady-state IR has shown that separate water subensembles exist in Nafion, and the relative populations are dictated by the overall water content of the membrane.[31,32] Recent ultrafast IR experiments in sodium-substituted Nafion have shown that the orientational relaxation time of water increases dramatically as the hydration is reduced.[32,33] Unfortunately, IR studies of protonated Nafion are not feasible due to the polarizability of hydronium, which swamps the entire mid-IR spectral window, and a molecular probe must be used to extract dynamics on a microscopic level.

In this paper, the nature of proton transfer in three separate regions of Nafion is studied. Three molecular probes are used that are sensitive to the local proton concentration. As will be demonstrated below using fluorescence anisotropy measurements, each probe is located in a different region of the hydrophilic domain. The three probes are shown in Figure 1. The molecule 8-hydroxypyrene-1,3,6-trisulfonate (HPTS) carries three negative charges in its ground electronic state, which makes it highly hydrophilic. The high negative charge density of HPTS results in Columbic repulsion with the sulfonic acid terminated side chains of Nafion and forces HPTS to reside in the aqueous water regions of the channels. Consequently, when Nafion is at sufficiently high hydration, HPTS experiences a water environment that is similar to bulklike water. The preference of HPTS to reside in the aqueous regions results in the molecule undergoing free orientational diffusion in Nafion with large water content, as observed in a previous study.[25] Rhodamine 6G (R6G) is also water-soluble like HPTS, but it carries a positive charge. Rhodamine's cationic charge produces an electrostatic attraction with the sulfonic acid side chains and results in R6G residing in close contact with the water−polymer interface. R6G's close proximity to the negatively charged interfacial region was first suggested by Hatrick et al. from observing dramatically slowed orientational diffusion of the molecule in Nafion relative to bulk water.[34] The experiments presented here show the anisotropy decay is biexponential and much slower than R6G's anisotropy decay in bulk water even at the highest water content in Nafion. The biexponential anisotropy decay at high water concentration is discussed in terms of the wobbling-in-a-cone model,[35] in which orientational relaxation is inhibited by R6G's interactions with the interface. The amide derivative of HPTS, 8-hydroxy-*N*,*N*,*N*′,*N*′,*N*′′,*N*′′-hexamethylpyrene-1,3,6-trisulfonamide or HPTA, is nonpolar and only sparingly soluble in water. The low solubility of HPTA causes the probe molecule to be embedded in the hydrophilic−hydrophobic boundary of the sulfonic acid and pendant side chain region that separates the water channels from the hydrophobic fluorocarbon region. HPTA's location inside the interfacial region of Nafion is supported by a complete lack of orientational diffusion of the probe molecule at all hydration levels, as shown experimentally later in this paper.

The three probe molecules provide information on distinct aspects of proton transfer in Nafion channels. The proton transfer kinetics of HPTS in protonated Nafion at maximum hydration are identical to the kinetics displayed by HPTS in a 0.5 M HCl solution. The hydronium concentration near the water interface of Nafion is estimated to be 1.4 M from the experiments with rhodamine-6G. These results are in contrast to the supposition that hydrated Nafion is a "superacid." Excited state proton transfer (ESPT) is followed in the nonpolar side chain regions of Nafion with the photoacid HPTA. Excited state proton transfer of HPTA is possible in protonated Nafion only at the highest hydration level.

II. Experimental Procedures

Rhodamine (Eastman Kodak), 8-hydroxypyrene-1,3,6-trisulfonic acid trisodium salt (Fluka), and 8-hydroxy-*N*,*N*,*N*′,*N*′,*N*′′,*N*′′-hexamethylpyrene-1,3,6-trisulfonamide (Fluka) were all used as received. Nafion 117 membranes were purchased from Fuelcellstore.com in the acid form.

The Nafion samples imbedded with HPTS or R6G were prepared by first soaking the Nafion membrane for 1 h in a 1 M HCl solution, which is sufficient to fully protonate the membrane,[36] followed by a deionized water rinse. HPTS was incorporated into Nafion by boiling the membrane in a ∼0.1 M solution of HPTS for 24 h. R6G was incorporated by soaking Nafion in a 10^{-5} M solution for 24 h at room temperature. After the probe molecules were incorporated in the membrane, the samples were again soaked in 1 M HCl for 1 h and rinsed with deionized water to ensure the sulfonic acid groups were protonated.

Due to the poor solubility of HPTA in water, HPTA was dissolved in a 1:1 mixture of water and methanol. Nafion was soaked in a $\sim 10^{-4}$ M HPTA solution overnight. The Nafion membrane was then rinsed with water for 4 h. For the protonated Nafion samples, the Nafion membrane with HPTA incorporated was soaked in 1 M HCl for 24 h and rinsed with deionized

water. For the sodium-substituted Nafion samples, the membranes were instead soaked in 1 M NaCl for 24 h and rinsed with deionized water.

A home-built humidity system was used to control the hydration level of the Nafion samples. First the samples with the chromophore already incorporated were dried. Then, air, with relative humidity that can be adjusted from 0 to 100%, was circulated through a sealed Plexiglas box. An internal humidity meter was used measure the relative humidity level, which was kept constant. The number of water molecules per sulfonate, λ, was determined by measuring the mass uptake of Nafion as a function of relative humidity.

Fluorescence spectra were taken on a Fluorolog-3 fluorescence spectrometer. UV−vis measurements were taken on a Cary-3 spectrometer. Attenuated total reflectance spectra were taken with a Vertex 70 FT-IR spectrometer with a diamond internal reflection crystal.

The time-correlated single photon counting (TCSPC) spectrometer used has been described elsewhere.[25] The TCSPC measurements for excited-state proton transfer dynamics were made by rotating the polarization of the excitation beam to the magic angle (54.7°) with respect to the collecting polarizer. The anisotropy measurements were carried out by setting the excitation polarization to 0° and 90° to measure the parallel and perpendicularly polarized fluorescence decays, denoted as $I_{||}(t)$ and $I_{\perp}(t)$, respectively. The time-dependent polarized fluorescence intensities can be expressed as

$$I_{||}(t) = P(t)(1 + 0.8C(t)) \quad (1)$$

$$I_{\perp}(t) = P(t)(1 - 0.4C(t)) \quad (2)$$

where $P(t)$ is the excited-state population decay and $C(t)$ is the second Legendre polynomial dipole orientational correlation function. Orientational relaxation can be separated from the population dynamics by defining the time-dependent anisotropy as

$$r(t) = \frac{I_{||}(t) - I_{\perp}(t)}{I_{||}(t) + 2I_{\perp}(t)} = 0.4C(t) \quad (3)$$

since $P(t) = I_{||}(t) + 2I_{\perp}(t)$. The 0.4 prefactor occurs for perfectly polarized absorption and emission spectra. In general the prefactor is <0.4.

III. Results and Discussion

1. Water Core. The probe molecule HPTS is highly soluble in water, and it carries a large −3 formal charge that repels the sulfonic acid functional groups lining the wall of the hydrophilic domains of Nafion. At high hydration levels, the sulfonic acid groups are ionized to generate anions, which increase the electrostatic repulsion between the HPTS probe and the boundary of the hydrophilic domains.

Evidence of HPTS residing in the interior of the water pools is given by the anisotropy decay curves shown in Figure 2. The qualitative behavior demonstrated in Figure 2 is very similar to a previous study of the methoxy derivative of HPTS, MPTS, in Na-Nafion.[25] At very low hydration (the $\lambda = 1$ decay curve), HPTS is virtually immobilized due to confinement in very small channels or the absence of water altogether. As water is added to the Nafion membrane, the hydrophilic domains grow in size and allow HPTS to rotate more freely causing the fluorescence

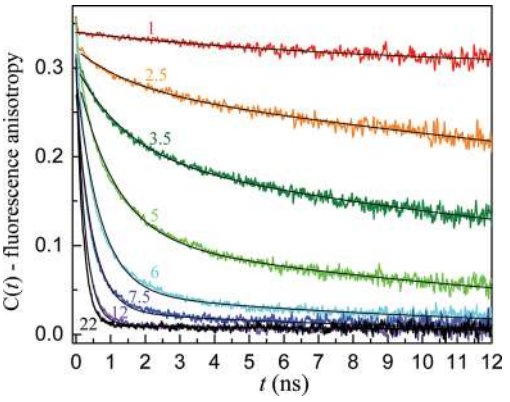

Figure 2. Anisotropy decays (colored curves) and fits (black curves) of HPTS in the water nanopools of Nafion.

TABLE 1: HPTS in Nafion Anisotropy Decay Parameters

λ	a_1	τ_1 (ns)	a_2	τ_2 (ns)
1	0.04	9.5	–	–
2.5	0.04	1.6	0.28	50
3.5	0.10	1.5	0.20	28
5	0.19	1.1	0.11	16
6	0.24	0.7	0.05	12
7.5	0.25	0.5	0.03	9
12			0.30	0.26
22			0.30	0.20
bulk			0.36	0.16

anisotropy to decay more rapidly. With the maximum amount of water added to Nafion, $\lambda = 22$, the anisotropy decay rate of HPTS is almost the same as that observed for HPTS in bulk water. At moderate to high hydration levels ($\lambda > 7.5$), the anisotropy decay curves fit well to a single-exponential that decays fully to zero. However, as the water pools become smaller, the anisotropy decays cannot be fit with a single exponential but rather fit reasonably well to biexponentials. Fitting parameters for the hydration range studied are given in Table 1. a_i is the amplitude of the ith decay component, and τ_i is the corresponding decay constant. The transition from a single-exponential to a biexponential anisotropy decay at $\lambda = \sim 7.5$ was reported previously for MPTS in Na-Nafion.[25]

The anisotropy decay time of HPTS in $\lambda = 22$ H-Nafion is 19% slower than the value measured in bulk water. The nearly identical MPTS molecule was previously measured to have an anisotropy decay time in AOT at $\lambda = 20$ that is 17% slower than in bulk water.[25] These results demonstrate a rough equivalence between the AOT and Nafion systems at the same hydration. It is therefore reasonable to assume there exists a similar effective volume of water surrounding HPTS in $\lambda = 22$ H-Nafion as in an AOT reverse micelle of comparable water content. The sizes of AOT reverse micelles are well characterized by a variety of methods.[26−28,37] AOT reverse micelles are monodispersed and well modeled as spherical. At $\lambda = 22$, an AOT reverse micelle water pool is ~7.5 nm,[26] which can serve as a rough approximation for the general size of the water pool accessible to HPTS. The largest dimension of the HPTS molecule is approximately 1 nm. Therefore, the large water pools will not restrict the rotational movement of HPTS, and single-exponential orientational randomization kinetics are reasonable.

It was previously found for MPTS in AOT reverse micelles that the reorientational kinetics are not single exponential when λ is 6 or less, which is consistent with observations in both sodium and protonated Nafion.[25] At a water content of $\lambda = 6$,

the water pool of an AOT reverse micelle is 2.8 nm in diameter.[26] As the diameter of the water pool approaches the molecular size of the imbedded chromophore, orientational relaxation slows dramatically, and complete orientational randomization may not be possible.

The multiexponential anisotropy decay of MPTS in Na-Nafion was interpreted in terms of a wobbling-in-a-cone model,[35] which is used here to discuss the orientational motion of HPTS in protonated Nafion. With wobbling-in-a-cone, orientational relaxation occurs on two time scales. On the faster time scale, physical restrictions result in orientational diffusion that can only sample a limited cone of angles. If the orientational constraints relax, then on a longer time scale complete orientational relaxation will occur.

When two statistically independent processes lead to orientational relaxation, in this case a fast wobbling-in-a-cone process and a longer time-scale process responsible for complete orientational randomization, the total correlation function can be expressed as a product of two independent correlation functions. The result is a biexponential decay. In Table 1, τ_1 is associated with the wobbling motion, and τ_2 arises from the longer time scale complete randomization of the orientation. In this picture, the irregular hydrophilic channels of Nafion restrict the orientational motion of HPTS on a short time scale. However, on a longer time scale, HPTS is able to sample a larger section of orientational space through random fluctuations of the polymer matrix and also translational motion that allows HPTS to move past some of the obstacles that restrict the molecule's orientational motion.

The biexponential nature of the anisotropy decay of HPTS in Nafion under low hydration levels might be attributed to the heterogeneity of the hydroscopic domains in the polymer. However, the fact that the orientational relaxation of MPTS in AOT reverse micelles is very similar to its behavior in Na-Nafion argues strongly in favor of the wobbling mechanism to explain the biexponential decays at low water content. AOT reverse micelles are monodispersed in size. Therefore, heterogeneity cannot be the explanation for the biexponential decays observed in the reverse micelles. Given the similarity in the orientational relaxation dynamics in AOT reverse micelles and in Nafion, it is highly unlikely that two distinct mechanisms would account for the biexponential decays in the two types of systems.

The anisotropy of HPTS in Nafion at maximum hydration ($\lambda = 22$) indicates the water environment surrounding the chromophore is very similar to bulk water. The decay is a single exponential, and no wobbling component is evident. It was previously observed by time-resolved infrared experiments that the orientation relaxation and hydrogen bond dynamics of water in AOT reverse micelles with a water content larger than $\lambda = 20$ behave very much like bulk water except for water molecules at the surfactant interface.[38−40] The relatively small difference in HPTS anisotropy decay times between $\lambda = 22$ Nafion and bulk water may be due to HPTS not residing precisely in the center of the water pool. Electrostatic screening is expected to be significant in the water pool due to a high ionic strength, which could allow some of the anionic HPTS molecules to approach close enough to the negatively charged sulfonate interface to contact the restricted boundary layer water. Regardless, the effects of confinement on HPTS orientational motion appear to be small at high levels of hydration, even at $\lambda = 12$, approximately half of the maximum hydration level. The motion of HPTS is largely unrestricted, and the local environment can be approximated as bulk water.

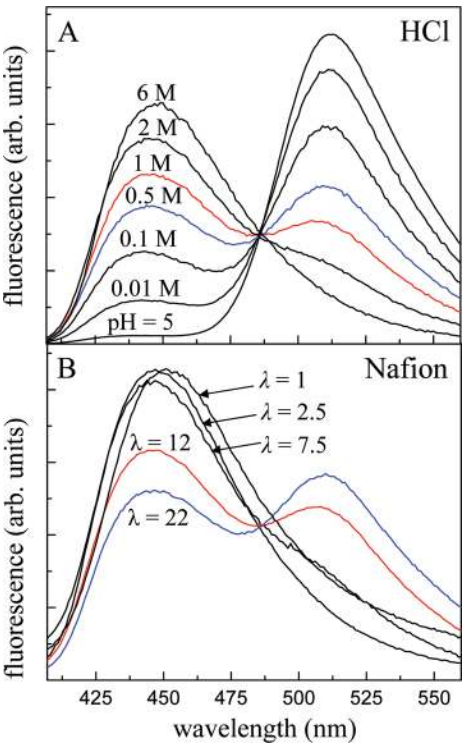

Figure 3. (A) Fluorescence spectra of HPTS in solutions of HCl. (B) Fluorescence spectra of HPTS in Nafion. The 0.5 and 1 M curves in A are colored to match the $\lambda = 22$ and 12 curves in B for comparison.

In Table 1, the last three rows, $\lambda = 12$ and 22, and bulk water, have a single decay constant because their decays are single exponentials. There is no wobbling component because there are no slowly relaxing constraints to reorientation. Beginning with $\lambda = 7.5$, there are two time constants. The wobbling time constant, τ_1, for $\lambda = 7.5$ is slower than the higher water content single exponential decay constants. The wobbling time constant slows as the hydration level is reduced. For $\lambda = 1$, only a single time constant is listed as the wobbling time constant. The decay is very slow, and it is possible that the orientation does not fully randomize on any time scale. It was not possible to obtain orientational relaxation data at sufficiently long time to determine if there is a very slow component associated with complete randomization. It is possible that complete randomization does not occur. The amplitude of the wobbling component decreases substantially as the hydration level is reduced. The amplitude of the wobbling component is related to the cone angle of the restricted motion.[41] A smaller value of a_1 corresponds to a smaller cone angle. For $\lambda = 7.5$, the cone angle is large. As the hydration level decreases, the range of angles sampled on the faster time scale decreases. In addition, the decay time for the slow component (complete orientational randomization) becomes increasingly long. The values of 28 and 50 ns for $\lambda = 3.5$ and 2.5, respectively, are approximate because the time range over which the decays can be determined is limited by the excited state lifetime. However, the qualitative trends are clear. As the hydration level is reduced, orientational relaxation is more constrained, and the relaxation of the constraints slows.

As discussed in the Introduction, HPTS is acidic in the excited state ($pK_a^* = 1.3$)[42] and readily undergoes proton transfer in an aqueous environment. Figure 3A shows the fluorescence spectra of HPTS in water with a range of HCl concentrations. The fluorescence spectra consist of a combination of peaks representing the protonated state (445 nm) and the deprotonated

state (510 nm). The dynamics of ESPT for HPTS in water are very fast (~90 ps) relative to the excited state lifetime (~5 ns), and in nonacidic aqueous solutions the molecule fluoresces almost entirely from the deprotonated state.[43,44] As the aqueous proton concentration increases, the ratio of fluorescence from the deprotonated state to fluorescence from the protonated state decreases. At a proton concentration of 6 M, HPTS fluoresces virtually entirely from the protonated state.[45]

The fluorescence spectra of HPTS in protonated Nafion are shown in Figure 3B. Even at the highest hydration level, there is a significant amount of fluorescence from the protonated state. The anisotropy decay dynamics indicate that the water environment surrounding HPTS at $\lambda = 22$ closely resembles that of bulk water. Therefore, the presence of fluorescence from the protonated state at the highest hydrations can be attributed to a pH effect and is not due to geometrical aspects of the water pool. The effective pH in Nafion at $\lambda = 22$ is estimated by comparing the ratio of fluorescence amplitude at 445 and 512 nm, $F_{445/512}$, with the fluorescence amplitude ratio of HPTS in solutions of different acid concentrations (Figure 3A). The 0.5 M spectrum in Figure 3A ($F_{445/512} = 1.12$) is very similar to the $\lambda = 22$ spectrum in Figure 3B ($F_{445/512} = 1.08$). The proton concentration in Nafion at $\lambda = 22$ is calculated to be 0.54 M. From the definition of $\lambda = 22$, there are 22 water molecules for every sulfonic acid unit. If it is assumed that the density of water is unchanged from the bulk value and all of the acidic protons are ionized and evenly distributed throughout the solution, then the proton concentration would be ~2.5 M, which is a factor of 5 greater than the observed value.

The wall of the water pool is negatively charged, and the hydronium counterions may tend to stay near the sulfonate surface. Counter ions situated in the vicinity of the negatively charged interface experience a very large electrostatic attraction compared with the thermal energy, k_BT, and these counterions are referred to as being condensed on the polyelectrolyte surface. The condensation appears as a double layer consisting of an interfacial and diffuse ion layer.[46] The fraction of counterion condensation, α, can be roughly estimated by approximating the size of the water pools in Nafion to that of AOT reverse micelles at the same hydration. In this approximation, α is ~80%. This number is most likely an upper limit to the condensation as it assumes all sulfonic acid groups inhabit a water cluster region. In actuality, some sulfonic acids will remain separated from the ionic clusters due to entropy requirements of the polymer network and will lower the true value of α somewhat. Nevertheless, the estimated value of α is entirely reasonable when compared to the measured condensation values of alkali metal dodecyl sulfate micelles,[47] which serve as a model system for the sulfonate−water boundary in Nafion. Lithium is the best alkali metal to represent hydronium, and Li^+−dodecyl sulfate micelles have a 70% condensation.

The amount of ESPT, indicated by the fluorescence spectra, decreases rapidly as the Nafion membrane is dehydrated (see Figure 3B). The reduction in proton transfer has two probable causes. First, as the water pools become smaller, the number of acidic sulfonic groups remains the same, but the number of water molecules is diminished. The concentration of protons naturally increases, and the aqueous environment becomes more acidic. In this respect, the shift in proton transfer equilibrium in Nafion is equivalent to that observed by changing the acid concentration in bulk water as shown in Figure 3A. In reducing the size of the water pool from $\lambda = 22$ to $\lambda = 12$, the anisotropy decay of HPTS only varies slightly, suggesting the water environment surrounding the photoacid still behaves approximately like free water. In this scenario, one can expect the concentration of aqueous protons to double as the water volume is halved. The estimated free proton concentration from the fluorescence spectrum at $\lambda = 12$ is 0.95 M. The observed change in acidity relative to $\lambda = 22$ is close to what is predicted (~1 M) from the volume reduction.

From Figure 3B, it can be seen that HPTS hardly undergoes any ESPT in $\lambda = 7.5$ protonated Nafion; the deprotonated fluorescence band is very small. It was previously shown in Na-Nafion that the finite size of the nanoscopic cavity can dramatically slow down the rate of proton transfer due to confinement effects of the surrounding water.[25] Significant changes in the extent of ESPT in Na-Nafion were observed for λ less than 8, which were also observed in AOT reverse micelles with the same water content. The anisotropy decay of HPTS in protonated Nafion becomes biexponential at $\lambda = 7.5$, and the time scale increases rapidly relative to bulk water as the hydration level is decreased. These observations demonstrate that the restrictions due to nanoconfinement are also important in H-Nafion as λ falls under approximately 8. If the fluorescence spectrum of HPTS in protonated Nafion at $\lambda = 7.5$ is related to a titration curve, as done for $\lambda = 22$ and 12, the estimated proton concentration would be 4.2 M. A concentration of 4.2 M would be over 4 times the calculated proton concentration in Nafion at $\lambda = 12$, but the difference in the amount of water between the two hydrations is less than a factor of 2; clearly the dramatic reduction in ESPT observed in $\lambda = 7.5$ is not solely due to the increasing concentration of protons as the cavity size is reduced. The slowing of the dynamics of water observed in Na-Nafion and AOT reverse micelles also plays a role.[38]

As discussed for the $\lambda = 22$ hydration, the concentration profile of protons in the water pools of Nafion is not expected to be homogeneous throughout the water pool. Condensation of counterions is known to form on charged surfaces to create an electrical double layer.[48] As the size of the water pool shrinks, the probe molecule will reside in closer proximity to the boundary layer, and the local concentration of protons will increase. The reduced ESPT that occurs at $\lambda = 7.5$ compared to higher hydration levels is likely caused by a combination of restrictions placed on the hydrogen bonding network of water due to confinement[38] and because the HPTS molecule must reside near the interfacial water layer, which has an increased concentration of protons due to electrostatic interactions.

No significant amount of ESPT is visible for HPTS in H-Nafion for λ less than 7.5. At the lowest water contents, the fluorescence spectrum of HPTS shifts to longer wavelengths. Reducing the water content in Na-Nafion results in a shift to shorter wavelengths for HPTS due to the environment's reduced ability to solvate the molecule in the excited state.[25] The hydrogen bond donating ability of the solvent has a large influence on the fluorescence spectrum of HPTS.[49] The negative charges on HPTS are stabilized through hydrogen bond interactions with the surrounding solvent. Stronger hydrogen bonds make the sulfonates of HPTS better electron-withdrawing groups and increase the amount of excited state charge transfer, shifting the fluorescence spectrum to longer wavelengths. The red-shift of HPTS at the lowest hydration suggests that there is no water layer to provide separation between the molecule and the extremely strong hydrogen bond donating sulfonic acid groups at the aqueous boundary.

The proton transfer kinetics of HPTS have been extensively studied by TCSPC.[50−52] Due to the large attraction between the negatively charged HPTS anion and a positively charged dissociated proton, the molecule serves as a model system for

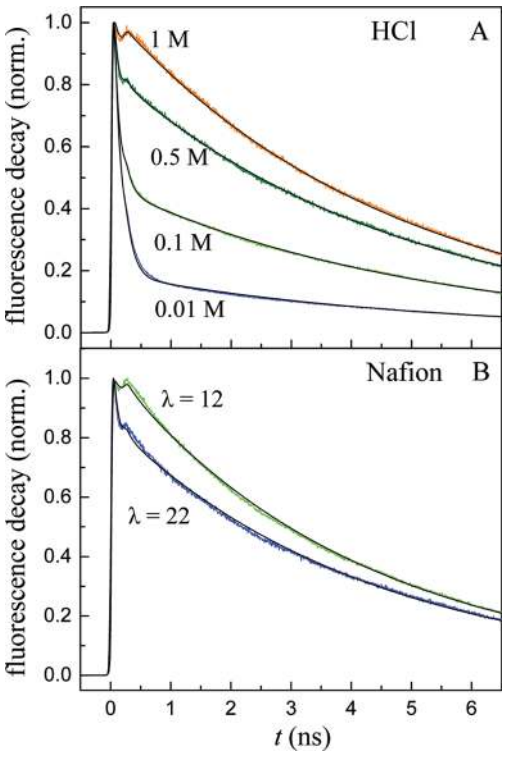

Figure 4. (A) Fluorescence decays at 445 nm of HPTS in HCl solutions (colored curves) with fits (black curves). (B) Fluorescence decays at 445 nm of HPTS in Nafion at high hydration levels (colored curves) with fits (black curves).

observing excited state geminate recombination.[50] At high acid concentrations, the effects of geminate recombination are hidden by the overwhelming number of protons in solution.[53,54] In a mineral acid solution at reasonably high concentrations (over 50 mM),[54] the fluorescence decay of the protonated state of HPTS is approximately biexponential. ESPT occurs on a short time scale, ~90 ps in neutral water,[43] and the protonated−deprotonated state populations will quickly come to an equilibrium determined by the surrounding proton concentration. Fluorescence of the protonated state will then decay with the excited-state lifetime of the molecule, which is ~5 ns in neutral water, but the lifetime is also pH dependent.

The fluorescence decay curves in Figure 4A of HPTS in aqueous HCl solutions taken at 445 nm fit well to a biexponential model after convolution with the instrument response. (Note, the short time peak that is apparent in some of the data comes from the instrument response and is reproduced by the convolution.) At acid concentrations larger than 1 M, the fast component due to ESPT is absent, in agreement with the fluorescence spectra in Figure 3A. The fluorescence kinetics of HPTS in H-Nafion with $\lambda = 22$ and 12 hydrations, along with fits to a biexponential model, are shown in Figure 4B for comparison. The $\lambda = 22$ decay constants roughly match the decay constants for 0.5 M HCl (see Table 2). Likewise, the $\lambda = 12$ decay constants resemble the decay constants for 1 M HCl. From the fitting parameters, at $\lambda = 22$ and 12 hydrations the extent of proton transfer is 44% and 22%, respectively, which correspond with the amplitudes of the protonated and deprotonated fluorescence seen in Figure 3B.

The kinetics of ESPT for $\lambda = 12$ are slightly slower than for $\lambda = 22$ (by a factor of 1.3), but the relative difference is in line with the difference in the anisotropy decay times of HPTS between the two samples. Furthermore, the difference in ESPT kinetics between the $\lambda = 22$ and 12 hydrations agree well with the difference in ESPT rates between $\lambda = 20$ and 10 AOT reverse micelles.[25] The fact that the proton transfer rate constants for $\lambda = 22$ and 12 are near the range measured in bulk water (~0.1 ns) supports the comparison of the highest hydration samples with bulk aqueous systems. For high acid concentrations, ESPT does not occur, and the fits become approximately single-exponential. In Nafion, the fits typically have a small biexponential component even when proton transfer is not present, but this may be associated with the heterogeneity of the water pools leading to a distribution of lifetimes. The lifetime of HPTS at the lowest hydration has a relatively large biexponential component, but this is most likely related to the extreme acidity the molecule encounters as it is solvated by sulfonic acid functional groups, which is evidenced by the perturbed fluorescence spectrum.

TABLE 2: (A) HPTS in H-Nafion Fluorescence Decay Parameters and (B) HPTS in HCl Solution Fluorescence Decay Parameters[a]

(A) λ	τ_1 (ns)	τ_2 (ns)	a
1	0.93	4.06	0.30
6	0.77	4.07	0.04
7.5	0.49	4.02	0.09
12	0.13	4.08	0.21
22	0.08	4.30	0.44
(B) [HCl]	**τ_1 (ns)**	**τ_2 (ns)**	**a**
0.01 M	0.11	4.97	0.89
0.1 M	0.09	5.01	0.73
0.5 M	0.07	4.78	0.47
1.0 M	0.08	4.64	0.23
2.0 M	1.06	4.40	0.02
6.0 M	1.99	4.18	0.03

[a] a is the amplitude of the τ_2 component, and $1 - a$ is the amplitude of the τ_1 component.

2. Water Interface. The negative charge of HPTS causes the molecule to reside in the center of the water pool. Conversely, R6G is a cation and has an affinity for the interfacial region, which is in close proximity to the negatively charged sulfonate groups. The ability of Nafion to immobilize cationic dyes has been used in previous photochemical studies.[55,56] The high uptake of R6G in Nafion due to its positive charge has led to the suggestion of using the chromophore as an in situ fluorescence sensor for fuel cell operation.[57,58]

Evidence for the association of R6G with the interfacial water region is given by the anisotropy dynamics shown in Figure 5. The functional form of the anisotropy decays are fit to a biexponential function, like for HPTS at mid-to-low hydration levels, and the fitting parameters are given in Table 3. At the maximum water content possible, $\lambda = 22$, the orientational relaxation occurs on a time-scale of nanoseconds. The anisotropy decay of R6G in bulk water (included in Figure 5 for comparison) is ~200 ps and single exponential. Unlike HPTS, which sits in the center of the water pool, as the aqueous domains grow in size the anisotropy decay time for R6G never approaches the rate of anisotropy decay in bulk water.

All of the decays for hydration levels greater than $\lambda = 5$ are very similar in shape and have a weighted-average anisotropy decay constant in the range of 12−16 ns. The decays for λ greater than 5 are also marked by complete orientational randomization of R6G at long times. The similarity in orientational dynamics at larger hydration levels suggests the

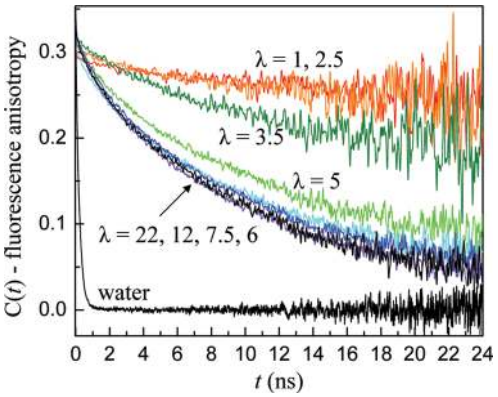

Figure 5. Anisotropy decays of R6G in Nafion and bulk water.

TABLE 3: Anisotropy Parameters of R6G and Local Proton Concentration in H-Nafion

λ	a_1	τ_1 (ns)	a_2	τ_2 (ns)	[H]
1	0.05	11.45	0.24	∞	7.7
2.5	0.06	6.08	0.25	∞	7.7
3.5	0.12	5.27	0.21	∞	5.8
5	0.20	8.65	0.10	82.2	3.5
6	0.11	5.05	0.18	22.9	2.5
7.5	0.08	3.25	0.23	16.5	1.8
12	0.08	3.57	0.22	14.6	1.4
22	0.15	6.08	0.15	18.7	1.4
bulk	0.32	0.20			

surrounding water environment in the area where R6G resides remains relatively constant as the size of the water pool is varied. This is unlike the results for HPTS, where the local viscosity of the inner water pools continuously decreases as the water pools grow in size.

As the hydration level drops below $\lambda = 5$, there is an abrupt change in the orientational kinetics of R6G. The anisotropy does not appear to decay to zero in the long time limit. As the water pool further reduces in size, shown by the $\lambda = 1$ and 2.5 decay curves, virtually all orientational diffusion stops for R6G. The sharp change in orientational diffusion for R6G at $\lambda \sim 3.5$ may be explained by the binding of cations to the sulfonate groups of Nafion. The sulfonate symmetric stretching mode of Nafion is sensitive to the proximity of the counterion. A contact ion pair between the sulfonate group and its counterion results in shifting the vibrational spectrum to higher frequencies.

The vibrational spectrum is displayed in Figure 6 with Li^+ chosen as the counterion. The vibrational spectrum red-shifts as water is added signifying the Li^+ cation is less tightly bound to the sulfonate group. The spectral shift continues until the

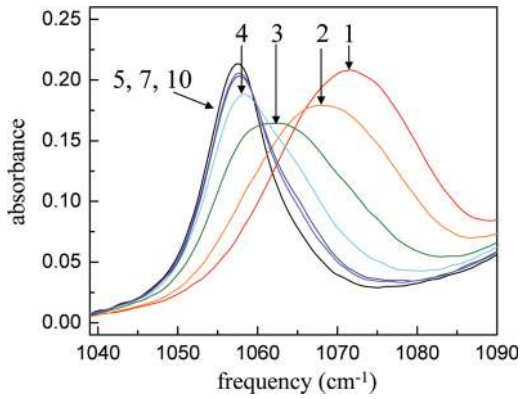

Figure 6. FT-IR spectra of Li-Nafion for various hydration levels.

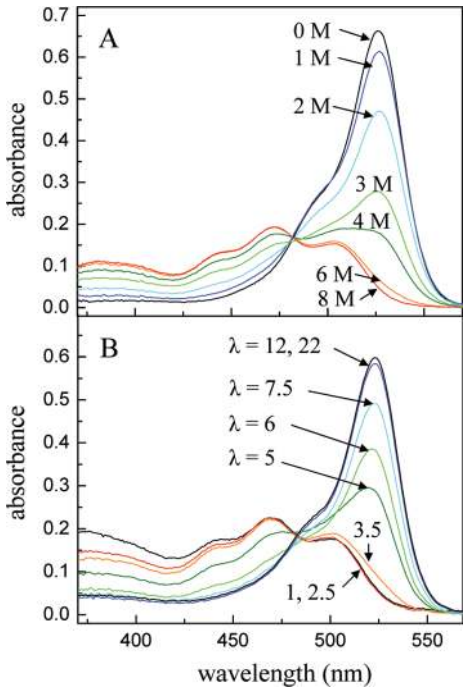

Figure 7. (A) Absorbance spectra of R6G in HCl solutions. (B) Absorbance spectra of R6G in Nafion.

hydration level is $\lambda \sim 3-4$, after which the vibrational spectrum is constant as more water is added. This evolution of the vibrational spectrum was previously observed by Lowery and Mauritz[59] using a series of alkali metals. They interpreted the results as arising from a change from a contact ion pair to the ions being separated by a water hydration layer. The results presented in Figure 6 show that approximately 3−4 water molecules per sulfonate group are required to form a hydration layer separating the two ions. Similar estimates of roughly 4 water molecules being required to solvate each sulfonate group have been made from the thermodynamics of the water uptake curve of Nafion.[3,8] R6G behaves much like a simple cation: at low hydrations, under $\lambda \sim 4$, R6G exists as a contact ion pair with the sulfonate ions. The formation of contact ion pairs explains why R6G is completely immobilized at $\lambda = 2$, but HPTS still enjoys some orientational freedom. As λ becomes larger than four, the R6G and sulfonate ions are separated by a solvation layer, but the ions stay in close proximity due to electrostatic forces.

One of the secondary amines of R6G (see Figure 1) can be protonated, and the molecule will be a +2 cation in highly acidic media. The proton transfer equilibrium of R6G is shown by the absorption spectra in Figure 7A where the molecule is titrated with HCl. The deprotonated state has an absorbance maximum at 527 nm, and the protonated state's maximum absorbance appears at 472 nm. The pK_a of R6G is reported as −0.38,[58] which agrees with the results given by Figure 7A.

The absorption spectrum of R6G in Nafion is highly dependent upon the membrane hydration, which has been reported by others.[57,58] The changes in the absorption spectrum of R6G in Nafion (Figure 7B) match the changes seen as R6G is titrated with HCl in bulk water (Figure 7A). Similar to the approach taken for HPTS, the local effective proton concentration experienced by the R6G molecule can be estimated by equating the absorption ratios taken at 440 and 527 nm, $A_{527/440}$, which are due to the protonated state and deprotonated state, respectively, in Nafion to the $A_{527/440}$ values obtained from the titration

curve of R6G. The computed effective proton concentrations are given in Table 3.

At maximum hydration, $\lambda = 22$, the proton concentration of the interfacial region is estimated to be 1.4 M. The interfacial proton concentration is nearly three times higher than in the water core region, which is 0.5 M as estimated using HPTS. A difference in acidity between the two regions is caused by the electrostatics of the charged interface that results in an ion gradient. A recent simulation of Nafion predicted that the free energy minimum of the solvent separated the hydronium−sulfonate head group ion pair to be 0.5−0.6 kcal/mol, which leads to a predicted proton concentration near the sulfonates to be a factor of 2−3 larger than in the middle of the hydrophilic domains.[16] As the water pool is reduced in volume by nearly a factor of 2 in going from $\lambda = 22$ to $\lambda = 12$, the proton concentration at the interface remains constant. In contrast, the proton concentration of the inner water region doubles as the volume is halved. The difference in the response of proton concentration to volume change in the two regions suggests that the water is primarily removed from the inner core as the hydration is reduced and the number of water molecules in the boundary layer remains constant. This result is not at all surprising considering the enthalpy of hydration of the sulfonate interface of Nafion is estimated to be three times more exothermic than the water core.[8]

R6G gives a more reliable estimate of proton concentration at low hydration levels because the measurement is made from the ground state and the kinetics of proton transfer do not interfere with observing equilibrium properties. The proton concentration increases sharply as the hydration falls below $\lambda = 12$. It is interesting to note that, in ultrafast infrared experiments, below a hydration of $\lambda = 10$ in AOT reverse micelle systems the dynamics of water start to show significant perturbations with respect to the micelle size, indicating that the "bulklike" core water has essentially disappeared.[38] On smaller length scales, the entire water pool is thought be coupled through the hydrogen bond network. By this comparison, it is very reasonable that the water boundary layer in Nafion is affected by a change in volume as the hydration becomes significantly less than $\lambda = 10$. It is still expected that there exists a hydration layer separating the hydronium ions from the sulfonate groups as long as λ is greater than four. The exact distance separating the ion pair is unknown, but state-of-the-art simulations of Nafion have predicted the radial distribution function of the oxygen atom in the hydronium ion and the oxygens in $-SO_3^-$ to be peaked at ~4 Å.[16]

The most dramatic change to the protonation state of R6G is witnessed for hydrations under $\lambda = 5$, which is a similar trend to what is observed for the anisotropy decay curves of R6G. As discussed in detail above, when there are less than four water molecules per sulfonate group, the positively charged counterions, including both R6G and hydronium ions, form contact ion pairs with the sulfonate groups. The sulfonate "wall" has a very high proton concentration, and the R6G probe experiences an extremely acidic environment.

3. Hydrophobic Wall. ESPT in the hydrophobic regions of the ionic cluster still accessible to water can be probed through the use of a nonionic molecule. The photoacid HPTA, which is the sulfonamide derivative of HPTS, is largely insoluble in water but has a similar change in pK_a upon excitation as HPTS. A detailed discussion of the electronic structure and photoacidity of HPTA relative to HPTS can be found elsewhere,[60] but for the purpose of this study, HPTA is slightly more acidic in the excited state (pK_a* = −0.7)[45] and the time scale from proton transfer in bulk water is 28 ps.[61]

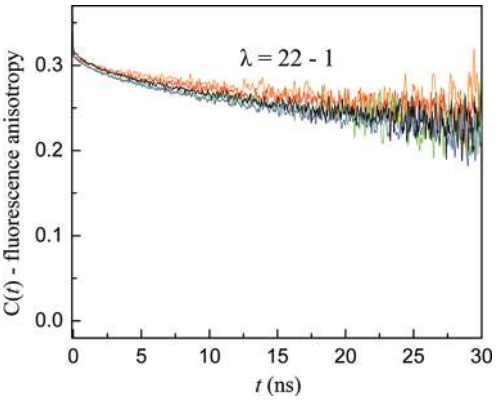

Figure 8. Anisotropy decays for HPTA in Nafion.

The preference for HPTA to reside in the wall of the water channels in Nafion is demonstrated by the anisotropy decay curves in Figure 8. The orientational dynamics are independent of the water content. Very little orientational relaxation occurs, regardless of the size of the water pool. If the anisotropy decay curves are fit to an exponential function with an offset and interpreted as a wobbling-in-a-cone process, then the average cone angle of diffusion is 25°. In contrast, the anisotropy decay of HPTS in Nafion at high hydrations exhibits free orientation diffusion, and the time scale approaches that observed in bulk water.

Even though the orientational dynamics of HPTA are not influenced by the water content in Nafion, the fluorescence spectrum and fluorescence decay kinetics are still affected by the amount of water present. The fluorescence spectra are displayed in Figure 9A. The protonated and deprotonated states of HPTA have maxima at 470 and 550 nm, respectively. At the highest water content, $\lambda = 22$, ESPT occurs to a small extent, as indicated by the appearance of the deprotonated peak. The deprotonated state disappears as the water content of the membrane is reduced. Only fluorescence from the protonated state is present for λ less than 12. The fluorescence spectrum red-shifts sharply as the hydration is lowered to $\lambda = 1$, with a fluorescence maximum at 510 nm. A shift in fluorescence to longer wavelengths was also observed for HPTS in H-Nafion at $\lambda = 1$ but to a much smaller extent than found for HPTA.

The fluorescence decay kinetics (population relaxation) of the protonated state (collected at 470 nm) are shown in Figure 9B. Only the $\lambda = 22$ and 1 curves are labeled. The curves between these two are $\lambda = 12$, 7.5, 6, 5, 3.5, and 2.5. ESPT reduces the protonated state lifetime. Although ESPT occurs to some extent at high hydration levels, as shown in Figure 9A, the fluorescence decays are the slowest for the samples with the greatest water content. The fluorescence lifetime decay curves fit to a biexponential decay with the parameters given in Table 4A. The excited state lifetimes of both time constants steadily decrease with decreasing water content. This trend is not surprising since a high proton concentration of the surrounding environment is known to shorten the excited state lifetime of many photoacid molecules.[62−64] Because ESPT is not important, particularly at the lower hydration levels, the biexponential decays suggest that there are two distinct environments for HPTA.

The fluorescence red-shift of HPTA at $\lambda = 1$ is unusual in magnitude. The red-shift of HPTS is a modest 5 nm in going from $\lambda = 2.5$ to $\lambda = 1$, but the red-shift for HPTA with the

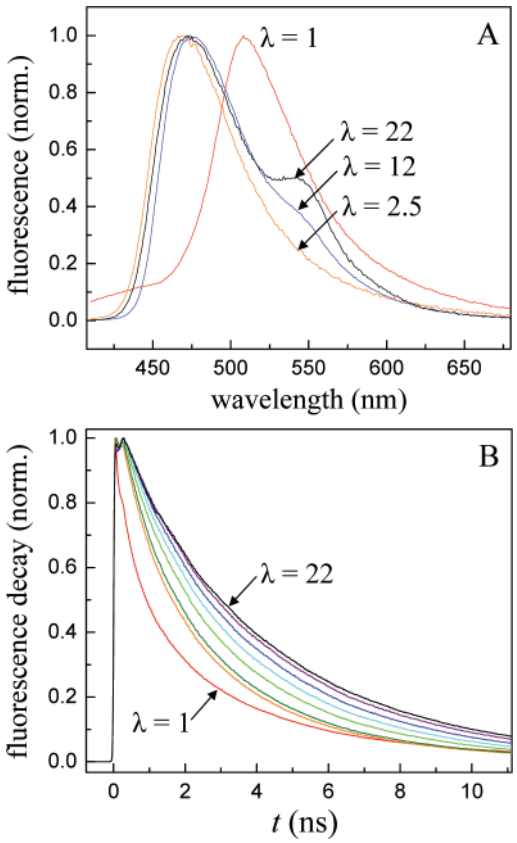

Figure 9. (A) Fluorescence spectra of HPTA in Nafion. (B) Fluorescence decays of HPTA in Nafion at 470 nm. The curves are for hydrations $\lambda = 22$, 12, 7.5, 6, 5, 3.5, 2.5, and 1.

TABLE 4: (A) Fluorescence Decay Parameters for HPTA in H-Nafion and (B) Fluorescence Decay Dynamics of HPTA in Na-Nafion[a]

(A) λ	τ_1 (ns)	τ_2 (ns)	a
1	0.86	4.32	0.57
2.5	1.20	3.63	0.50
3.5	1.28	3.63	0.46
5	1.59	3.87	0.40
6	1.85	4.06	0.35
7.5	2.01	4.23	0.28
12	2.07	4.43	0.22
22	1.79	4.54	0.15

(B) λ	$1/k_{pt}$ (ns)	$1/k_A$ (ns)	K	$1/k_B$
1		4.32		
2.5		4.12		
3.5		4.09		
5	1.16	4.06	0.07	7.99
6	1.03	4.14	0.15	7.43
9	0.93	4.16	0.29	7.47
17	0.72	3.75	0.42	7.26

[a] a is the amplitude of the τ_2 component, and $1 - a$ is the amplitude of the τ_1 component.

same hydration change is 40 nm. Charge transfer behavior has been noted to occur in HPTA that may result in the formation of a charge transfer state in extreme solvating environments.[60] Charge transfer is not possible for HPTS. At $\lambda = 1$, the solvating environment in the ionic clusters of Nafion is expected to resemble pure sulfonic acid. Indeed, when HPTA is dissolved in water−methylsulfonic acid mixtures, the same trend in

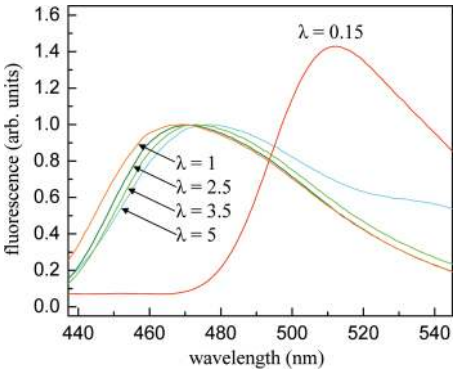

Figure 10. Fluorescence spectra of HPTA in methylsulfonic acid−water mixtures.

fluorescence is seen (Figure 10) as in H-Nafion. The methylsulfonic acid is akin to the solvation environment created by the sulfonic acid units in Nafion. As the number of waters per methylsulfonic acid, which is still denoted as λ, becomes smaller, there is a blue-shift in the fluorescence of the protonated state. The blue-shifting trend with decreasing water content is observed until λ becomes significantly smaller than one. However, when λ becomes very small, as seen in the $\lambda = 0.15$ fluorescence spectrum, a large red-shift in the spectrum occurs, and the shape and position match what is seen in Nafion at $\lambda = 1$ (Figure 9A). The discontinuous change in the fluorescence shift, first moving toward shorter wavelengths, then a dramatic change to longer wavelength as the water content becomes sufficiently small, suggests a separate electronic state is responsible. The equivalence of the fluorescence spectra of HPTA in Nafion at $\lambda = 1$ and in nearly pure methylsulfonic acid suggests HPTA has an environment that is very similar to concentrated sulfonic acid, and it is not substantially exposed to the fluorocarbon backbone or the ether side chains of the Nafion matrix.

The local proton concentration experienced by HPTA cannot be estimated from matching the fluorescence spectrum in Nafion with a point on the titration curve taken in bulk solution. The dynamics of water are severely restricted at all hydration levels at the interface and the less polar regions occupied by HPTA. Recent time-resolved infrared experiments have been able to separate the dynamics of water in the interior water pool from the interface in AOT reverse micelles,[39] which should give an estimate of the time scale for water reorganization in the different regions of Nafion. It was found, at higher hydration levels, that the reorientational dynamics of water in the core regions were like bulk water (~2 ps), but the interfacial water's orientational motion was slower by an order of magnitude (~18 ps).

The probe molecule may also be inhomogeneously distributed in the Nafion membrane. The ESPT kinetics depend upon the availability of water to accept a proton. Because HPTA sits in a relatively hydrophobic area of the cavity, the local water concentration could be highly variable. In addition, the orientation of HPTA as it is imbedded in the stationary wall also affects the kinetics of proton transfer. If the hydroxyl end of HPTA faces inward toward the interface, it is unlikely that the photoacid will be hydrogen bonded to a water molecule in an appropriate configuration to facilitate proton transfer.

HPTA was incorporated in Na-Nafion to eliminate the effects of a large proton concentration on the ESPT process. Excited state deprotonation of HPTA occurs to a much larger extent in Na-Nafion, as seen in the fluorescence spectra in Figure 11A.

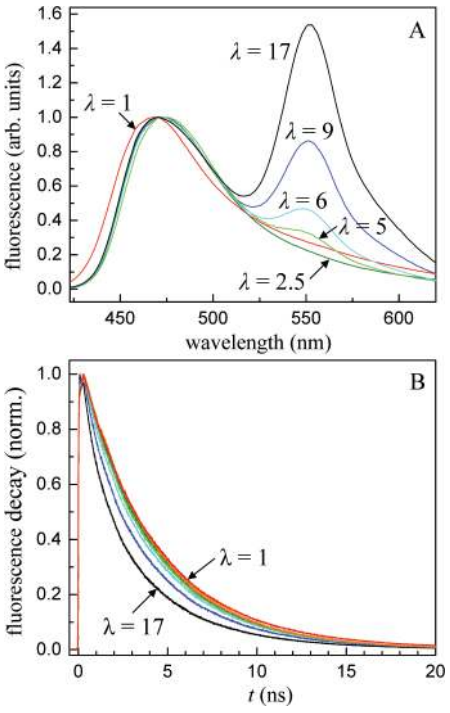

Figure 11. (A) Fluorescence spectra of HPTA in Na-Nafion. (B) Fluorescence decays of HPTA in Na-Nafion at 470 nm. The curves are for hydrations $\lambda = 17$, 9, 6, 5, 3.5, 2.5, and 1.

Fluorescence from the deprotonated state, peaked at 550 nm, first appears at $\lambda = 5$ and steadily grows as the water content increases. At the maximum hydration of Na-Nafion, $\lambda = 17$, much more fluorescence from the deprotonated state is present relative to fully hydrated H-Nafion, $\lambda = 22$, even though the total amount of water in the sodium substituted form is lower.

The relationship between the excited state population decay of the protonated state and water content in Na-Nafion (Figure 11B) is reversed from what is observed in H-Nafion: as the H-Nafion membrane is hydrated, the population decay of the protonated state becomes faster. Only the $\lambda = 17$ and 1 curves are labeled. The curves between these two are $\lambda = 9$, 6, 5, 3.5, and 2.5. The increasing decay of the protonated state as the water pools grow in size is primarily due to ESPT. The lowest hydration samples, $\lambda = 1$, 2.5, and 3.5, do not undergo ESPT. The fluorescence dynamics describing the protonated and deprotonated populations are fit to a kinetic model. The proton transfer rate constant is k_{pt}. To fit the data, it is necessary to include a parameter K, which is the fraction of the HPTA molecules that are able to undergo ESPT.

$$A(t) = (K\exp(-k_{pt}t) + 1 - K)\exp(-k_A t) \quad (8)$$

$$B(t) = \frac{k_{pt}K}{k_{pt} + k_A - k_B}(1 - \exp(-(k_{pt} + k_A - k_B)t))\exp(-k_B t) \quad (9)$$

The equations for $A(t)$ and $B(t)$ describe the populations of the photoacid and conjugate base pair, respectively, that have fluorescence decay rates of k_A and k_B.

The parameters extracted from simultaneously fitting the excited state populations of the protonated (470 nm) and deprotonated (550 nm) states of HPTA are listed in Table 4B. Sample fits for $\lambda = 9$ are shown in Figure 12. The proton transfer time is 720 ps at the highest hydration level, which

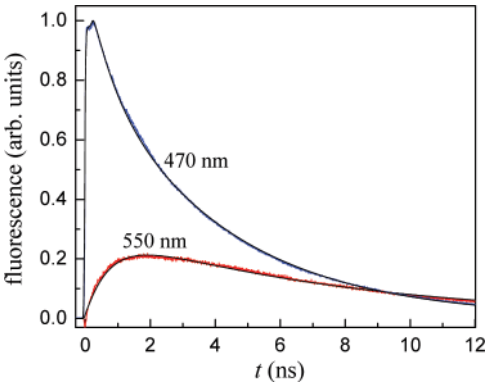

Figure 12. Kinetic model fits (black curves) to fluorescence decays (colored curves) of HPTA in Na-Nafion for $\lambda = 9$ at 470 nm (protonated state) and 550 nm (deprotonated state).

is a factor of 24 slower than the proton transfer time in bulk water. The proton transfer time increases as the size of the water domains shrinks. However, the overall increase is much smaller than observed for HPTS proton transfer in the inner water pools.[25] The rather modest change in proton transfer kinetics with respect to the water content may be related to the dynamics of water molecules at the interface. The water dynamics are controlled by the ionic sulfonate groups, which have a similar influence on neighboring water molecules at all hydrations.

The fraction of HPTA chromophores able to undergo proton transfer, represented by K, disappears as the Nafion membrane loses water. As suggested by the lack of decay of the anisotropy (Figure 8), the HPTA molecule cannot translate on the time scale of the excited state lifetime. Therefore, a water molecule must exist in the immediate vicinity of HPTA to accept a proton for ESPT to occur. Penetration of water into the sulfonate region, and even further into the ether side chains, is dependent on the water content of the membrane. At maximum hydration, ~40% of the HPTA molecules can undergo ESPT. This number, which is related to the water content in the nonpolar regions of the ionic cavity, diminishes as water is removed from the membrane and is negligible for λ less than four.

IV. Concluding Remarks

Proton transfer dynamics and equilibrium proton concentrations vary greatly in different areas of the water pools of Nafion as observed by molecular probes. The center of the water pools, which were studied with the highly anionic molecule HPTS, behave very much like bulk water when the membrane is well hydrated, that is, for λ greater than 12. With high hydration, the proton transfer kinetics of HPTS in Nafion are almost the same as measured in bulk solution. The proton concentrations in the center of the water pools of Nafion with hydrations of $\lambda = 22$ and $\lambda = 12$ were calculated to be 0.54 and 0.95 M, respectively.

Time-resolved fluorescence anisotropy measurements indicate that as the water content of the membrane drops below $\lambda = \sim 8$ the water environment surrounding the HPTS probe becomes significantly different from bulk water conditions. Anisotropy dynamics for HPTS in protonated Nafion were found to be very similar to a previous study in Na-Nafion as well as in AOT reverse micelles. HPTS excited state proton transfer does not occur when λ is less than 8 due to the encroachment of the molecule on the interfacial water region, which has a significantly higher proton concentration due to

electrostatic interactions. The water hydrogen bond dynamics also slow significantly when λ is less than 8, as shown by previous ultrafast IR experiments.[38] The slower water dynamics hinder the proton transfer process. Under hydration levels of $\lambda \sim 3.5$, HPTS cannot undergo complete orientational diffusion indicating the hydrophilic region has dimensions similar to the size of the probe molecule (~1 nm).

The cationic probe R6G samples the water environment near the sulfonate decorated interface in the Nafion channels. R6G experiences a much more acidic environment than HPTS due to the boundary layer formed by hydronium ions in the negatively charged interfacial region. At the highest hydration levels, the effective proton concentration felt by R6G is 1.4 M, which is nearly a factor of 3 higher than in the water core. The orientational dynamics of R6G are unaltered as the hydration is varied for $\lambda = 22$ to 6, indicating the water environment at the interface is fairly constant in this hydration range. Below $\lambda = 5$, there is an abrupt change in the orientational motion of R6G as the water solvation layer surrounding the molecule is eliminated, and R6G forms contact ion pairs with the immobile sulfonate groups. The value of λ where the transition in orientational dynamics for R6G occurs is very near the point where a longtime offset appears in the anisotropy decay of HPTS. The fact that total orientational relaxation is obstructed at the same λ suggests the two molecules inhabit a similar domain below $\lambda \sim 5$. The contact ion equilibrium observed for R6G agrees with the behavior of simple alkali cations as shown by FT-IR spectroscopy. As R6G comes in direct contact with the sulfonate−sulfonic acid layer, the absorption spectrum shows that R6G is completely in the protonated state, which indicates a very acidic environment.

Proton transfer dynamics at the hydrophobic−hydrophilic boundary are monitored with the neutral HPTA photoacid. Orientational dynamics indicate HPTA is immobile at all hydration levels on the time scale of the fluorescence lifetime. The environment surrounding HPTA does however depend upon the amount of water in the membrane, as demonstrated by the fluorescence spectrum and lifetime kinetics. ESPT is observable in the fluorescence spectrum only at the highest water content. Both a high proton concentration and hindered water dynamics reduce the amount of ESPT. The same experiments in Na-Nafion show that proton transfer is possible at the interface to a significant extent (42% of the HPTA molecules undergoing ESPT at the highest hydration), but the kinetics are dramatically slowed relative to bulk conditions because of the restricted nature of water at the interface.

Acknowledgment. This work was supported by the Department of Energy (DE-FG03-84ER13251). D. B. Spry thanks the National Science Foundation for an NSF Fellowship.

References and Notes

(1) Mauritz, K. A.; Moore, R. B. *Chem. Rev.* **2004**, *104*, 4535.
(2) Anantaraman, A. V.; Gardner, C. L. *J. Electroanal. Chem.* **1996**, *414*, 115.
(3) Zawodzinski, J. T. A.; Derouin, C.; Radzinski, S.; Sherman, R. J.; Smith, T. V.; Springer, T. E.; Gottesfeld, S. *J. Electrochem. Soc.* **1993**, *140*, 1041.
(4) Hsu, W. Y.; Gierke, T. D. *Macromolecules* **1982**, *15*, 101.
(5) Gierke, T. D.; Munn, G. E.; Wilson, F. C. *J. Polym. Sci., Polym. Phys.* **1981**, *19*, 1687.
(6) Roche, E. J.; Pineri, M.; Duplessix, R. *J. Polym. Sci., Polym. Phys.* **1982**, *20*, 107.
(7) Yeager, H. L.; Steck, A. *J. Electrochem. Soc.* **1981**, *128*, 1880.
(8) Duplessix, R.; Escoubes, M.; Rodmacq, B.; Volino, F.; Roche, E.; Eisenberg, A.; Pineri, M. *Water in Polymers*; ACS Symposium Series No. 127, Washington, DC, 1980.
(9) Cappadonia, M.; Erning, J. W.; Stimming, U. *J. Electrochem. Soc.* **1994**, *376*, 189.
(10) Litt, M. H. *Polym. Prepr.* **1997**, *38*, 80.
(11) Rieberer, S.; Norian, K. H. *Ultramicroscopy* **1992**, *41*, 225.
(12) Ceynowa, J. *Polymer* **1978**, *19*, 73.
(13) Xue, T.; Trent, J. S.; Osseo-Asare, K. *J. Membr. Sci.* **1989**, *45*, 261.
(14) Petersen, M. K.; Wang, F.; Blake, N. P.; Metiu, H.; Voth, G. A. *J. Phys. Chem. B* **2005**, *109*, 3727.
(15) Blake, N. P.; Petersen, M. K.; Voth, G. A.; Metiu, H. *J. Phys. Chem. B* **2005**, *109*, 24244.
(16) Petersen, M. K.; Voth, G. A. *J. Phys. Chem. B* **2006**, *110*, 18594.
(17) Allahyarov, E.; Taylor, P. L. *J. Phys. Chem. B* **2009**, *113*, 610.
(18) Devanathan, R.; Venkatnathan, A.; Dupuis, M. *J. Phys. Chem. B* **2007**, *111*, 13006.
(19) Cwirko, E. H.; Carbonell, R. G. *J. Membr. Sci.* **1992**, *67*, 227.
(20) Urata, S.; Irisawa, J.; Takada, A.; Shinoda, W.; Tsuzuki, S.; Mikami, M. *J. Phys. Chem. B* **2005**, *109*, 4269.
(21) Cui, S.; Liu, J.; Selvan, M. E.; Paddison, S. J.; Keffer, D. J.; Edwards, B. J. *J. Phys. Chem. B* **2008**, *112*, 13273.
(22) Petersen, M. K.; Hatt, A. J.; Voth, G. A. *J. Phys. Chem. B* **2008**, *112*, 7754.
(23) Eisenberg, A.; Kim, J.-S. *Introduction to Ionomers*; Wiley: New York, 1998.
(24) Gebel, G. *Polymer* **2000**, *41*, 5829.
(25) Spry, D. B.; Goun, A.; Glusac, K.; Moilanen, D. E.; Fayer, M. D. *J. Am. Chem. Soc.* **2007**, *129*, 8122.
(26) Zulauf, M.; Eicke, H.-F. *J. Phys. Chem.* **1979**, *83*, 480.
(27) Magid, L. J.; Daus, K. A.; Butler, P. D.; Quincy, R. B. *J. Phys. Chem.* **1983**, *87*, 5472.
(28) Eicke, H.-F.; Kubik, R.; Hammerich, H. J. *J. Colloid Interface Sci.* **1982**, *90*, 27.
(29) Choppin, G. R. *J. Mol. Struct.* **1978**, *45*, 39.
(30) Pimentel, G. C.; McClellan, A. L. *The Hydrogen Bond*; W. H. Freeman and Co.: San Francisco, 1960.
(31) Falk, M. *Can. J. Chem.* **1980**, *58*, 1495.
(32) Moilanen, D. E.; Piletic, I. R.; Fayer, M. D. *J. Phys. Chem. A* **2006**, *110*, 9084.
(33) Moilanen, D. E.; Piletic, I. R.; Fayer, M. D. *J. Phys. Chem. C* **2007**, *111*, 8884.
(34) Hatrick, D. A.; Black, I.; Holmes, A. S.; Birch, D. J. S.
(35) Lipari, G.; Szabo, A. *J. Am. Chem. Soc.* **1982**, *104*, 4546.
(36) Zawodzinski, J. T. A.; Springer, T. E.; Davey, J.; Jester, R.; Lopez, C.; Valerio, J.; Gottesfeld, J. *J. Electrochem. Soc.* **1993**, *140*, 1981.
(37) Kinugasa, T.; Kondo, A.; Nishimura, S.; Miyauchi, Y.; Nishii, Y.; Watanabe, K.; Takeuchi, H. *Colloids Surf., A - Physicochem. Eng. Aspects* **2002**, *204*, 193.
(38) Piletic, I. R.; Moilanen, D. E.; Spry, D. B.; Levinger, N. E.; Fayer, M. D. *J. Phys. Chem. A* **2006**, *110*, 4985.
(39) Moilanen, D. E.; Fenn, E. E.; Wong, D.; Fayer, M. D. *J. Phys. Chem. B.* **2009**, ASAP.
(40) Moilanen, D. E.; Fenn, E. E.; Wong, D.; Fayer, M. D. 2009, ASAP.
(41) Lipari, G.; Szabo, A. *Biophys. J.* **1980**, *30*, 489.
(42) Rappoport, Z. *The Chemistry of Phenols*; Wiley, 2003.
(43) Pines, E.; Huppert, D. *J. Chem. Phys.* **1986**, *84*, 3576.
(44) Spry, D. B.; Goun, A.; Fayer, M. D. *J. Phys. Chem. A* **2007**, *111*, 230.
(45) Spry, D. B.; Fayer, M. D. *J. Chem. Phys.* **2008**, *128*, 084508.
(46) Lyklema, J. *Fundamentals of Interface and Colloid Science*; Academic Press: London, 1991.
(47) Joshi, J. V.; Aswal, V. K.; Goyal, P. S. *J. Phys.: Condens. Matter* **2007**, *19*, 196219.
(48) Russel, W. B.; Saville, D. A.; Schowalter, W. R. *Colloidal Dispersions*; Cambridge University Press: New York, 1989.
(49) Spry, D. B.; Goun, A.; Fayer, M. D. *J. Chem. Phys.* **2006**, *125*, 144514.
(50) Pines, E.; Huppert, D. *Chem. Phys. Lett.* **1986**, *126*, 88.
(51) Agmon, N.; Pines, E.; Huppert, D. *J. Chem. Phys.* **1988**, *88*, 5631.
(52) Elsaesser, T.; Bakker, H. J. *Ultrafast Hydrogen Bonding Dynamics and Proton Transfer Processes in the Condensed Phase*; Kluwer Academic Publishers: Dordrecht, The Netherlands, 2002.
(53) Gepshtein, R.; Leiderman, P.; Genosar, L.; Huppert, D. *J. Phys. Chem. A* **2005**, *109*, 9674.
(54) Solntsev, K. M.; Huppert, D.; Agmon, N. *J. Phys. Chem. A* **2001**, *105*, 5868.
(55) Mohan, H.; Moorthy, P. N.; Iyer, R. M. *Photochem. Photobiol.* **1989**, *49*, 395.
(56) Mika, A. M.; Lorenz, K.; Szczurek, A. *J. Membr. Sci.* **1989**, *41*, 163.

(57) Patil, Y. P.; Seery, T. A.; Shaw, M. T.; Parnas, R. S. *Ind. Eng. Chem. Res.* **2005**, *44*, 6141.
(58) Mohan, H.; Iyer, R. M. *Analyst* **1993**, *118*, 929.
(59) Lowery, S. R.; Mauritz, K. A. *J. Am. Chem. Soc.* **1979**, *102*, 4665.
(60) Spry, D. B.; Fayer, M. D. *J. Chem. Phys.* **2007**, *127*, 204501.
(61) Pines, E.; Pines, D.; Ma, Y.-Z.; Fleming, G. R. *ChemPhysChem* **2004**, *5*, 1315.
(62) Webb, S. P.; Phillips, L. A.; Yeh, S. W.; Tolbert, L. M.; Clark, J. H. *J. Phys. Chem.* **1986**, *90*, 5154.
(63) Harris, C. M.; Selinger, B. K. *J. Phys. Chem.* **1980**, *84*, 1366.
(64) Agmon, N. *J. Phys. Chem. A* **2005**, *109*, 13.

JP9036777